Author draft, IEEE Trans on Antennas and Propagation, VOL. 62, NO. 12, DECEMBER 2014, pp. 6501-6505, DOI 10.1109/TAP.2014.2360550

New Approaches and Algorithms for the Analysis of Vertical Refractivity Profile below 1 km in a Subtropical Region

A. AbouAlmal, R.A. Abd-Alhameed, S.M.R. Jones and H. AlAhmad

Abstract — **In this paper, 17 years of high resolution surface and radiosonde meteorological data from 1997-2013 for the subtropical Gulf region are analysed. Relationships between the upper air refractivity, N_h, and vertical refractivity gradient, ΔN, in the low troposphere and the commonly available data of surface refractivity, N_s are investigated. A new approach is discussed to estimate N_h and ΔN from the analysis of the dry and wet components of N_s, which gives better results for certain cases. Results are compared with those obtained from existing linear and exponential models in the literature. The investigation focusses on three layer heights at 65 m, 100 m and 1 km above ground level. Correlation between the components of N_s with both N_h and ΔN are studied for each atmospheric layer. Where high correlations were found, empirical models are derived from best-fitting curves.**

Index Terms – **Standard atmosphere, radio refractive index, microwave links, refractivity gradient**.

I. INTRODUCTION

Microwave line-of-sight links are designed taking into account the curvature of rays in a stratified atmosphere over the curved earth [1, 2]. Variation of atmospheric parameters such as temperature and relative humidity dominate the vertical refractivity profile. The prevailing meteorological conditions in a specific region determine the extent of refraction. Statistical analysis of refractivity and its vertical profile are essential to the prediction of fading and anomalous propagation, such as sub- or super-refraction and ducting, as well as interference probabilities from reliable surface and upper-air meteorological data. The extent of ray-curvature is determined by the gradient of the refractive index, in N-units, versus height in km from the surface. This is known as the surface lapse rate, ΔN. The ITU has defined a reference atmosphere in the form of a negative exponential model and proposed a reference value of -40 N/km for the vertical ΔN over the first kilometer in temperate regions [3]. ITU has also published global contour maps for the refractive index at Earth's surface, N_s, and ΔN at specified altitudes [2].

It has been noted that surface meteorological data are widely available and the information about N_s is more readily available than the upper air refractivity, N_h [4]. The shortage of upper air data can be attributed to the operational and maintenance cost of radiosonde ascents compared with fixed surface weather stations. Some linear and exponential models [2, 4, 5] have been proposed to predict N_h at height h and vertical ΔN from the available N_s data, where upper air data are not available. It has been noted that most of these relations, in particular for ΔN, are derived from the refractivity analysis at the ground and 1 km height. Several refractivity studies are available, e.g. [6-11], while only a few are available for the Arabian Gulf region [12-16], where high incidence of anomalous propagation conditions are reported.

The vertical refractivity profile in the first few hundred meters of the atmosphere, where terrestrial communication systems operate, is important for the analysis of these anomalous phenomena. In this study, the relationships and correlation between dry, wet and net components of N_s with the corresponding components of either N_h or ΔN are investigated at 65 m, 100 m and 1 km layers above the ground, which are common reference altitudes proposed by ITU [2]. To the best of our knowledge, the curve fitting analysis of the dry and wet components at each layer has not been reported before. Cumulative distributions and scatter diagrams are presented. New relationships are derived from the best fitting curves and compared with existing models.

Long-term radiosonde data recorded at Abu Dhabi, the capital of UAE, from two daily ascents, nominally at 00:00 and 12:00 UT, have been used for the analysis corresponding to 4:00 am and 4:00 pm local time. In certain periods, only one ascent was available per day, usually at 00:00 UT. More details about the radiosonde and the special climate of Arabian Gulf area were recently introduced in [12]. In this paper, the measured refractivity parameters, N_s, N_h and ΔN, refer to the values obtained from the surface and radiosonde meteorological measurements, whereas predicted values of N_h and ΔN refer to those calculated from the measured N_s using the models in sections I.A and I.B. The measured ΔN is derived from the measured N_s and N_h parameters using the linear model. Root mean square errors, RMSE, and correlation between the measured parameters and between measured and predicted values are presented, using the formulations as defined in MATLAB R2009a.

A. Refractivity Models

The atmospheric radio refractivity, N, at any altitude is calculated from the meteorological measurements of total atmospheric pressure (hPa), water vapor pressure (hPa) and absolute temperature (K) using the well-known refractivity formula [2, 5]. The N parameter consists of two components, N_D and N_W, which are often referred to as the dry and wet air contributions to refractivity [5]. The dry component contributes around 60 to 80 % of the overall value [9]. The ITU provide a reference atmosphere for terrestrial paths in the form of a negative exponential model for prediction of N_h at any height h (km) above mean sea level [2]:

$$N_h = N_0 \cdot e^{\left(\frac{-h}{h_0}\right)} \qquad (\mathrm{N-units}) \tag{1}$$

where N_o is refractivity extrapolated to sea level and ho is the height coefficient which is referred to by ITU as the scale height of the model. The ITU provides global maps of N_o

Abdulhadi AbouAlmal is with Engineering Department, Emirates Telecommunication Corporation, Etisalat, UAE (e-mail: eng_abdulhadi@yahoo.com).

Abdulhadi AbouAlmal, R.A.A. Abd-Alhameed and S.M.R. Jones are with the Antenna and Applied Electromagnetics Research Group, School of Electrical Engineering and Computer Science Bradford University, Bradford, West Yorkshire, BD7 1DP, UK (e-mail: r.a.a.abd@bradford.ac.uk).

Hussein AlAhmad is with Electrical Engineering Department, Khalifa University of Science, Technology & Research, Sharjah, UAE.

(derived using ho = 9.5 km) and proposes an average global profile based on N_o and h_o, values of 315 N-units and 7.35 km, respectively [2, 5]. It has been noted [2] that h_o may vary from one region to another.

Other relationships have also been proposed to predict N_h from the surface data [4, 5]. The following exponential model is further generalized to predict N_h from N_s considering "bulk" refractive index structure as opposed to short period random disturbances resulting from a variety of stochastic atmospheric processes [5]:

$$N_h = N_s \cdot e^{\left[-\left(\frac{h-h_s}{h_o}\right)\right]} \quad (\mathrm{N-units}) \tag{2}$$

B. *Refractivity Gradient Models*

The variation of ΔN is a function of climate, season, transient weather conditions across the day, clutter and terrain over the communication path. In the standard atmosphere, N_h decreases with altitude since the total pressure decreases more rapidly than temperature with height [17]. The vertical ΔN usually has a negative value causing the rays to bend towards the earth and to propagate beyond the geometric horizon. ΔN can be obtained from two refractivity values, N_s at the surface, h_s, and N_h at an altitude h, using the linear model, by dividing the refractivity difference (N_s - N_h) over (h_s - h) [5, 12, 18].

A close correlation has been observed between N_s and ΔN "near the ground", i.e. over the first few kilometers [5]. Several empirical equations have been derived to predict long-term mean values of ΔN for the first kilometer layer of atmosphere above the ground from measured N_s parameter, which are only applicable to average negative gradients close to the surface [4, 5]. If N_h is not readily available, the refractivity gradient near the Earth's surface can be predicted either by differentiating (2), [5] or by applying the linear model for the measured N_s and the predicted N_h. Other models are also studied to predict the vertical ΔN near the ground from the measurements of electromagnetic wave strength and diffraction losses [19, 20]. For higher altitudes, different functions may be fitted as proposed by the three-part reference atmosphere model in Bean and Thayer's 1959 paper [5], which gives different expressions for the refractivity in the first kilometer, between 1 and 9 km and above 9 km. This has a drawback of introducing discontinuities in the ΔN profile. An exponential equation can also be used to directly relate ΔN with N_s as follows [4, 5]:

$$\Delta N = -a \cdot e^{(k \cdot N_s)} \ (\mathrm{N/km}) \tag{3}$$

where a and k are the model coefficients. Another exponential decaying relationship, obtained from curve fitting analysis between N_s and ΔN, was proposed for the first kilometer, $\Delta N_{1\mathrm{km}}$, [5, 15] as follows:

$$\Delta N_{1\mathrm{km}} = a \cdot (1 - e^{-bN_s})^c \quad (\mathrm{N/km}) \tag{4}$$

where a, b, and c are the model coefficients, which are found to be -477.45, 0.00736, and 22.297, respectively, in this study. In general, the values of coffecients of all the models are found to vary from one climate to another.Analyzing data for long periods may also provide more accurate values of the coeffecients. In order to extend these relations to other regions around the world, the correlation between long-term measured and predicted refractivity parameters need to be evaluated as well.

II. Analysis and Results

Seventeen years of high resolution meteorological data from 1997 till end of October 2013 have been analyzed in this study. Due to low quality or incomplete ascents, data for June 1998, April 2000, November 2005, June 2006 to November 2006 and January 2010 to May 2010 are not available. From December 2006 to December 2008, the data of only one ascent, mostly at 00:00 UT, is available on daily basis. In addition, a small number of abnormal values have been excluded owing to faulty readings from the instrument.

Two approaches, direct and indirect, have been used to predict N_h and ΔN from the measured N_s values. In the direct approach, N_h and ΔN are directly predicted from measured N_s using the linear or exponential models. A new indirect approach is proposed by analyzing the dry and wet components of the refractivity parameters using various prediction models. In this indirect approach, the dry and wet components of N_h or ΔN are first estimated from corresponding components of measured N_s based on the correlations observed between different components. Then, the net values of the predicted parameters, $\Delta N_{(\mathrm{D+W})}$ and $N_{h\_(\mathrm{D+W})}$, are computed by summing both dry and wet terms.

A. *ΔN Analysis at 65 m, 100 m and 1 km Layers*

The measured refractivity, N, has been evaluated from the radiosonde measurements at the ground and at the three specified altitudes. Then, the measured ΔN is obtained from the measured N_s and N_h for each layer using the linear model. In Figs. 1 and 2, the average seasonal and yearly variations of ΔN over the whole period of study are shown for each of the three layers. The mean monthly variations are significant for all the layers, as shown in Fig. 1. The gradient values at the 1 km layer, $\Delta N_{1\mathrm{km}}$, vary between -51 and -99 N/km, whereas the gradients span from -68 to -158 N/km and from -68 to -156 N/km, in case of the 100 m layer, $\Delta N_{0.1\mathrm{km}}$, and the 65 m layer, $\Delta N_{0.065\mathrm{km}}$, respectively. The range of variation is found to be approximately 45 units for $\Delta N_{1\mathrm{km}}$, 90 units for $\Delta N_{0.1\mathrm{km}}$ and 88 units for $\Delta N_{0.065\mathrm{km}}$.

Gradient values are lower (i.e. higher in magnitude, but negative) during summer months, May and June, than in winter months, January and December. This can be attributed to the decreasing vapor content and pressure with height and the observed temperature inversions (temperature increasing with height) during the night, particularly in summer. Such ΔN trends may explain the frequent interference cases even across national borders, which are commonly experienced by

terrestrial communication systems operating in the Gulf region during the summer months [12]. Occurrence of ΔN exceeding -100 N/km is related to the incidence of anomalous propagation [2, 6, 9, 12]. For ΔN_{1km}, no monthly mean is below -100 N/km, whereas $\Delta N_{0.1km}$ and $\Delta N_{0.065km}$ fall below this value for most months. In May, the monthly means of $\Delta N_{0.1km}$ and $\Delta N_{0.065km}$ even fall below the limit at which ducting phenomenon occurs, -157 N/km. The two peaks of $\Delta N_{0.1km}$ and $\Delta N_{0.065km}$ in October, where both monthly mean values of $\Delta N_{0.1km}$ and $\Delta N_{0.065km}$ are found to be higher than ΔN_{1km}, can be attributed to a bias in the data due to having only early-morning radiosonde data for this month. In 2007 and 2008, the data for October are only available for at 00:00 UT (4 am local time). In the morning, it is observed that the temperature and the water vapor pressure, *e*, often increase with altitude in many cases, in particular within the 65 m and 100 m layers, while *e* decreases considerably at 1 km height. The early morning/early evening effect on the gradient is clearly seen in the CDFs shown in Fig. 3. Consequently, the wet components of *N* and ΔN increase with altitude and ΔN attains large positive gradients in both 65 m and 100 m layers, which relates to the incidence of sub-refraction phenomenon [1, 6, 12]. The linear ΔN model has the drawback, particularly for the altitudes 100 m and below, that a small difference between the two refractivity values may result in large disagreement in ΔN due to the low decimal number in the equation's denominator. Also, the data for October 2006 were not available, which may also affect the overall result.

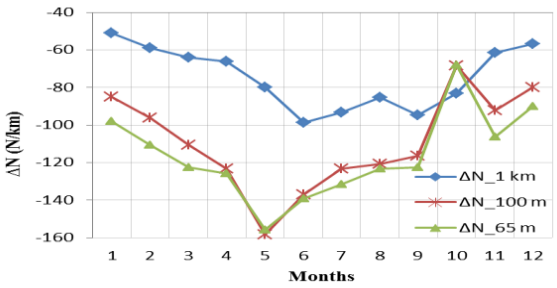

Fig. 1. Mean monthly variations of ΔN (1997 to Oct. 2013)

Year to year variation of the mean ΔN at 1 km, 100 m and 65 m, with spans of 32, 209 and 298 N-units, respectively, are given in Fig. 2. ΔN_{1km} shows no significant fluctuations, while the values of $\Delta N_{0.1km}$ and $\Delta N_{0.065km}$ fluctuate from -1.5 to -210 N/km, and from 31 to -267 N/km, respectively. It can be observed that the mean $\Delta N_{0.1km}$ and $\Delta N_{0.065km}$ values decreased for the four years 2002, 2003, 2004 and 2005, with some exceptional values in the years 2003 and 2004. One reason for such trend is the considerable decrement of the water vapor content and pressure with higher altitudes that were observed over the course of these years. This yearly increment could be part of some short-term climate cycle, although a cyclical pattern cannot be reliably inferred from the currently available measurements. By contrast, the mean ΔN over each of the three layers showed almost the highest values during 2010, which could be due to the missing five months data, in particular the months of April and May, which contribute to lower gradient values as shown above in Fig. 1.

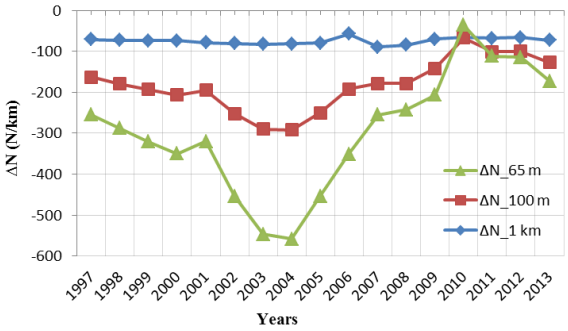

Fig. 2. Mean yearly variations of ΔN (1997 to Oct. 2013)

Cumulative distributions of ΔN_{1km}, $\Delta N_{0.1km}$ and $\Delta N_{0.065km}$ for different times of day over the whole period are shown in Fig. 3. The range of $\Delta N_{0.065km}$ varies between approximately -1947 and 1629 N/km, however only values between -1500 and 1500 N/km are displayed for clarity. The long-term mean values of ΔN_{1km}, $\Delta N_{0.1km}$ and $\Delta N_{0.065km}$ are -74.8, -109.6 and -116.4 N/km, respectively (well below the -40 of the ITU-R standard atmosphere), whereas the mean values at 00:00 and 12:00 UT are found to be -87.9 and -58.8 N/km for ΔN_{1km}, -138.7 and -74 N/km for $\Delta N_{0.1km}$, in addition to -134.9 and -93.7 N/km for $\Delta N_{0.065km}$.

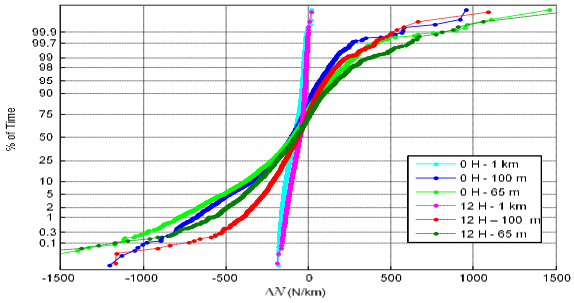

Fig. 3. Hourly Cumulative distributions of ΔN (1997 to Oct. 2013)

By comparing the 0 H and 12 H curves for each layer, it can be observed that the gradient values are lower during the morning. Meteorological phenomena following sunset, could be responsible for such a trend [9], where vapor content considerably decreases with height, particularly during the summer season, while in Winter the moisture content may increase with altitude leading to higher positive values of $\Delta N_{0.1km}$ and $\Delta N_{0.065km}$ than 12:00 UT. Similar results were also reported in a previous study [12], however over a shorter period of years.

B. Correlation of Refractivity Components

The models introduced in sections I (Parts A and B) for predicting N_h and ΔN parameters from measured N_s, are examined and the predicted results are compared in terms of RMSE and correlation with the measured N_h and ΔN parameters. Table 1 summarizes the results of RMSE and

correlation coefficients obtained for N_h and ΔN parameters using the exponential models (2) and (4), respectively, which give the best results in most cases, compared with other models. The h_o value is found to be 3.9 km, 3 km and 2.8 km for 1 km, 100 m and 65 m layers, respectively, for which minimum RMSE values can be obtained in each scenario. The exponential model (4) provides the best correlation and RMSE results for ΔN_{1km}, whereas (2) gives the best results of N_h at the 65 m and 100 m layers.

TABLE 1: CORRELATION AND RMSE VALUES OF EXISTING PREDICTION MODELS FOR N_h AND ΔN FROM N_s

Layer	N_h & ΔN	Correlation	RMSE
1 km	N_h	0.001	30.82
	ΔN_{1km}	0.86	18.77
100 m	N_h	0.87	15.18
	$\Delta N_{0.1km}$	0.29	151.7
65 m	N_h	0.91	12.59
	$\Delta N_{0.065km}$	0.24	196.2

No correlation has been found between N_h and N_s for the 1 km layer, while strong correlation is observed for the other two layers, 100 m and 65 m. On the other hand, the correlation between ΔN_{1km} and N_s exceeds 0.85, whereas it is found to be poor in case of the 65 m and 100 m layers. In addition, the correlation between the dry, wet and net components of measured N_s and the corresponding components of the measured N_h and ΔN are also investigated for each of the three layers. Table 2 provides the results of correlation matrix for all the scenarios. The dry component of N_s, N_{s_D}, is in good correlation with the dry component of N_h, N_{h_D}, at all altitudes, N_{1km_D}, $N_{0.1km\_D}$ and $N_{0.065km\_D}$, where the maximum correlation is observed within the 65 m layer. The N_{s_D} is found to be much less correlated with the dry components of ΔN in the three layers; ΔN_{1km_D}, $\Delta N_{0.1km\_D}$ and $\Delta N_{0.065km\_D}$. The wet component of N_s, N_{s_W}, is well correlated with the wet component of N_h at the 100 m and 65 m altitudes, $N_{0.1km\_W}$ and $N_{0.065km\_W}$, while it is found to be only correlated with the wet component of ΔN at the 1 km layer, ΔN_{1km_W}.

TABLE 2: CORRELATION MATRIX OF REFRACTIVITY COMPONENTS AT1 km, 100 m AND 65 m LAYERS

	N_s	N_{s_D}	N_{s_W}
N_{1km}	0.001		
N_{1km_D}		0.84	
N_{1km_W}			0.15
$N_{0.1km}$	0.874		
$N_{0.1km\_D}$		0.96	
$N_{0.1km\_W}$			0.89
$N_{0.065km}$	0.91		
$N_{0.065km\_D}$		0.97	
$N_{0.065km\_W}$			0.92
ΔN_{1km}	-0.85		
ΔN_{1km_D}		-0.56	
ΔN_{1km_W}			-0.86
$\Delta N_{0.1km}$	-0.30		
$\Delta N_{0.1km\_D}$		-0.55	
$\Delta N_{0.1km\_W}$			-0.29
$\Delta N_{0.065km}$	-0.26		
$\Delta N_{0.065km\_D}$		-0.54	
$\Delta N_{0.065km\_W}$			-0.25

In general, no correlation could be obtained between either dry or wet components of N_s, and ΔN at the 100 m and 65 m layers. It is also noted that the correlation between the net parameters follows the correlation between their wet components. These observations seem to be reasonable since the wet term of refractivity is proportional to the water vapor content that varies significantly across these layers, in particular within the layers close to the ground, and gets more stable at around 1 km height, while the dry term is proportional to the atmospheric pressure and inversely proportional to the dry temperature, which show less variation over all atmospheric layers within the first kilometer.

The slope of the vertical refractivity curve at 1 km, which refers to ΔN_{1km}, is correlated with N_s since the variation of N_{1km} is very small compared with $N_{0.1km}$ and $N_{0.065km}$, which are directly correlated with N_s. No correlation is observed between N_s and gradients at the layers close to the ground, $\Delta N_{0.1km}$ and $\Delta N_{0.065}$. Fig. 4 describes this phenomenon, where at 1 km height the refractivity value does not change significantly with the variations in N_s, while $N_{0.1km}$ and $N_{0.065km}$ vary significantly with N_s. The slope, ΔN, is only correlated with N_s in case of the 1 km layer, ΔN_{1km}, since N_{1km} is assumed to have a stable value while N_s varies between the states S1 and S2.

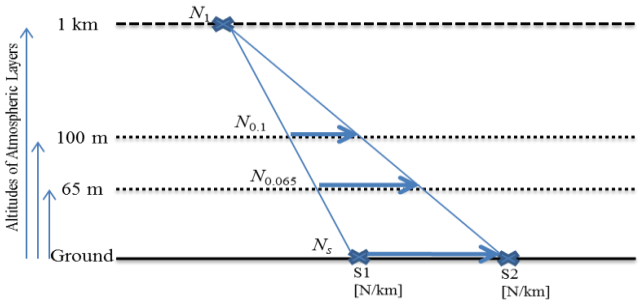

Fig. 4. Description of Correlation Between N_s, N_h and ΔN

C. Curve Fitting Analysis and Algorithms

The scatter diagrams of all measured refractivity parameters and components are studied. Some figures of the correlated parameters and components are provided and empirical algorithms are derived from the best fitting curves. All relationships are evaluated based on the determination coefficients, correlation of the obtained results with the measured data and RMSE values.

As presented in Table 2, the correlation between N_s and ΔN_{1km} is dominated by the wet components of the two parameters, N_{s_W} and ΔN_{1km_W}, while N_{s_D}, is found to be correlated with N_{1km_D} rather than ΔN_{1km_D}.

The scatter diagram between the wet components, N_{s_W} and ΔN_{1km_W}, is shown in Fig. 5. A third order polynomial relationship to predict ΔN_{1km_W} is obtained from the curve fitting analysis. The dry component of ΔN_{1km_D} is calculated

using the linear model from the predicted N_{1km_D} and measured N_{s_D}. N_{1km_D} is predicted from measured N_{s_D} using equation (2). This new indirect approach for predicting $\Delta N_{1km(D+W)}$ has less RMSE value than the direct approach for predicting ΔN_{1km} from measured N_s using the linear model, as shown in Table 3.

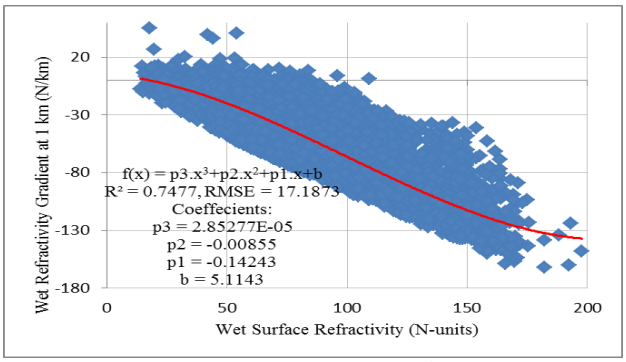

Fig. 5. Correlation between N_{s_W} and ΔN_{1km_W}

TABLE 3: COMPARISON OF TWO APPROACHES FOR ΔN_{1km} PREDICTION

	Correlation	**RMSE**
Direct Approach: ΔN_{1km} from measured N_s	0.85	30.8118
Indirect Approach: $\Delta N_{1km(D+W)}$ from Dry and Wet Components Analysis	0.85	19.3338

Multiple scatter diagrams are drawn for the dry, wet and net components of the measured N_h and ΔN against the corresponding measured N_s components at 65 m and 100 m atmospheric layers. Good correlation is observed between N_h and N_s components, while it is found to be poor between ΔN and N_s with large RMSE values obtained regardless of the approach or the prediction model to be used. This can be attributed to the sensitivity of ΔN to any small variation in the values of refractivity at these low altitudes. N_h has been predicted using the exponential model (2) considering both the direct and indirect approaches at the 65 m, $N_{0.065km}$, and 100 m, $N_{0.1km}$, layers. Due to the similarity of the N_h results at the 65 m and 100 m layers, the available data sets of these two layers are combined, $N_{0.065\&0.1km}$, to develop a single model for the atmospheric layers below 100 m altitude from the ground. The correlation and RMSE values of the measured and predicted N_h, N_{h_D}, N_{h_W} and $N_{h\_(D+W)}$, are compared for each of the three data sets at 65 m, 100 m and their combined set. For all scenarios, RMSE results for $N_{h\_(D+W)}$ using the indirect approach are better than the results of N_h obtained directly from the measured N_s, while correlation results are almost the same.

The scatter diagram of N_h against N_s is given in Fig. 6. Two exponential and third order polynomial relationships are obtained from the best fitting curves, which provide marginally better results in comparison with the other models. Both models have very similar results with marginal improvement for the polynomial model. However, the result from the polynomial is highly sensitive to the precision of the coefficients. The RMSE and correlation results obtained for the prediction of N_h from both direct and indirect approaches are similar. The following exponential model can be used for direct prediction of N_h below 100 m above the ground, where the values of the coefficients a and b are found to be 135.8 and 0.002609, respectively, for the area under study:

$$N_{0.065\&0.1km} = a \,.\, e^{(b \,.\, N_S)} \qquad (\mathrm{N-units}) \qquad (5)$$

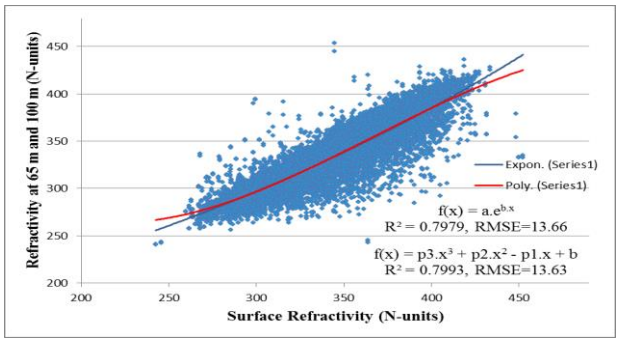

Fig. 6. Correlation between N_s and $N_{0.065\&0.1km}$

III. CONCLUSIONS

17 years of local radiosonde data from UAE were analysed to obtain the vertical refractivity profile for three critical atmospheric layers within the first kilometer above the ground. The correlation between N_s and either N_h or ΔN was found to depend predominantly on the wet components of these parameters.

For estimating ΔN at the three atmospheric layers, it was observed that the linear model resulted in somewhat lower RMSE values than the exponential one.

Based on the reduced RMSE, it is recommended to use the indirect approach to estimate N_h and ΔN from the analysis of dry and wet refractivity components, in particular at the 1 km layer. Marginal improvement was achieved for the 65 m and 100 m layers when N_h was predicted using the exponential model (2) based on the indirect approach. Such multi-steps analysis may lead to slightly lower correlation, when compared with the measured data, than using the direct relations.

Although the use of more than one model to predict the refractivity at different atmospheric layers may introduce some discontinuities in its vertical profile, the RMSE values of the predicted N_h or ΔN were found to be reduced while the correlation between the measured and predicted values was marginally improved for certain parameters.

Third- and fourth-order polynomial models showed marginal improvements in terms of RMSE and correlation values for the prediction of N_h and ΔN parameters over the other models. However, it was noted that the results were very sensitive to the precision of the high order coefficients.

ACKNOWLEDGMENT

The authors would like to express their gratitude to the National Center of Meteorology in UAE for providing the raw meteorological data used in this work, in addition to the

partial support from the Engineering and Physical Sciences Research Council (EPSRC), U.K., under Grant EP/E022936; and Technology Strategy Board of the Knowledge Transfer Programme KTP008734.

REFERENCES

[1] M. I. Skolnik, *Introduction to Radar Systems*, 3rd ed.: McGraw-Hill Inc., 2001.
[2] "ITU-R Recommendation P.453-10: The radio refractive index: its formula and refractivity data," *International Telecommunication Union*, 2012.
[3] "ITU-R Recommendation PN.310-9: Definitions of terms relating to propagation in non-ionized media," *International Telecommunication Union, ITU*, 1994.
[4] R. L. Freeman, *Radio System Design for Telecommunications*, 3rd ed.: John Wiley, 2007.
[5] "Handbook on Radiometeorology," *ITU R Bureau, International Telecommunication Union*, Geneva, 1996.
[6] T. G. Hayton and K. H. Craig, "Use of Radiosonde Data in Propagation Prediction," presented at the IEE, Savoy Place, London WC2R OBL, UK, 1996.
[7] L. S., "Investigation of surface refractivity and refractive gradients in the lower atmosphere of Norway," presented at the COST 235, CP 121, March 1993.
[8] A. K. P. Marsh, T. G. Hayton, and K. H. Craig, "Initial Comparison of Refractivity Parameters Derived from Radiosondes and Psychrometers in France," in *COST255, CP42010*, Oct. 1997.
[9] L. Blanchard and H. Sizun, "Refractivity Over France: First Results of ARGOS Experiment," *COST255, CP32003*, May 1997.
[10] K. H. Craig and T. G. Hayton, "Investigation of β0 values derived from ten years radiosonde data at 26 stations," presented at the COST 235, CP 182, Oct. 1993.
[11] K. H. Craig and T. G. Hayton, "Refractivity parameters from radiosonde data," in *AGARD Conference On Propagation Assessment in Coastal Environments*, Germany, 1994, pp. 1-12.
[12] A. AbouAlmal, R. A. Abd-Alhameed, K. Al-Ansari, H. Al-Ahmad, C. H. See, S. M. R. Jones, and J. M. Noras, "Statistical Analysis of Refractivity Gradient And β0 Parameter In The Gulf Region," *Antennas and Propagation, IEEE Transactions on*, vol. 61, pp. 6250-6254, 2013.
[13] Abdulhadi Abu Al-mal and K. Al-Ansari, "Calculation of Effective Earth Radius and Point Refractivity Gradient in UAE," *International Journal of Antennas and Propagation*, vol. 2010, 2010.
[14] Kifah Al-Ansari, Abdulhadi AbuAl-Mal, and R. A. Kamel, "Statistical Analysis of Refractivity in UAE," *Internationl Symposium on Rainfall Rate and Radiowave Propagation, India, Published by American Institute of Physics Conference Proceedings*, vol. 923, pp. 232-247, 2007.
[15] K. Al Ansari and R. A. Kamel, "Correlation Between Ground Refractivity and Refractivity Gradient and Their Statistical and Worst Month Distributions in Abu Dhabi," *Antennas and Wireless Propagation Letters, IEEE*, vol. 7, pp. 233-235, 2008.
[16] A. AbouAlmal, R. A. Abd-Alhameed, A. S. Hussaini, T. Ghazaany, Z. Sharon, S. M. R. Jones, and J. Rodriguez, "Comparison of Three Vertical Refractivity Profiles In The Gulf Region," in *Wireless Conference (EW), Proceedings of the 2013 19th European*, 2013, pp. 1-4.
[17] S. S. Mentes and Z. Kaymaz, "Investigation of Surface Duct Conditions over Istanbul, Turkey," *Journal of Applied Meteorology And Climatology*, vol. 46, 2006.
[18] Dominguez M. A., Benarroch A., and Riera J. M., "Refractivity Statistics in Spain: First Results," in *COST 255, CP52004*, May 1998.
[19] O. Jicha, P. Pechac, V. Kvicera, and M. Grabner, "Estimation of the Radio Refractivity Gradient From Diffraction Loss Measurements," *Geoscience and Remote Sensing, IEEE Transactions on*, vol. 51, pp. 12-18, 2013.
[20] O. Jicha, P. Pechac, V. Kvicera, and M. Grabner, "Estimation of radio refractivity profile gradient from multiple LOS links using artificial neural networks — First results," in *Antennas and Propagation (EUCAP), 2012 6th European Conference on*, 2012, pp. 1174-1177.